İSTANBUL TECHNICAL UNIVERSITY ★ INSTITUTE OF SCIENCE AND TECHNOLOGY

SURFACE IMPEDANCE RECONSTRUCTION

M.Sc. Thesis by

Gül Seda ÜNAL, B.Sc.

Department : **ELECTRONICS AND COMMUNICATION ENGINEERING**

Programme : **TELECOMMUNICATION ENGINEERING**

JUNE 2008

İSTANBUL TECHNICAL UNIVERSITY ★ INSTITUTE OF SCIENCE AND TECHNOLOGY

SURFACE IMPEDANCE RECONSTRUCTION

M.Sc. Thesis by

Gül Seda ÜNAL, B.Sc.

(504061334)

Date of Submission : 5 May 2008

Date of Examin : 11 June 2008

Supervisor : Prof. Dr. İbrahim AKDUMAN

Members of the Examining Committee Assoc. Prof. Dr. Ali YAPAR (İ.T.Ü.)

Asst. Prof. Lale Tükenmez ERGENE (İ.T.Ü.)

JUNE 2008

İSTANBUL TEKNİK ÜNİVERSİTESİ ★ FEN BİLİMLERİ ENSTİTÜSÜ

YÜZEY EMPEDANSI BELİRLENMESİ

YÜKSEK LİSANS TEZİ

Müh. Gül Seda ÜNAL

(504061334)

Tezin Enstitüye Verildiği Tarih : **5 Mayıs 2008**

Tezin Savunulduğu Tarih : **11 Haziran 2008**

Tez Danışmanı : **Prof. Dr. İbrahim AKDUMAN**

Diğer Jüri Üyeleri **Doç. Dr. Ali YAPAR (İ.T.Ü.)**

Yrd. Doç. Dr. Lale Tükenmez ERGENE (İ.T.Ü.)

HAZİRAN 2008

ACKNOWLEDGEMENT

I would like to thank Professor Doctor Ibrahim Akduman, who gave me the opportunity to work under his supervision, for his precious guidance and motivation in accomplishing this thesis study.

I also would like to express my gratitude to Associate Professor Doctor Ali Yapar who never hesitated to help me when I needed his assistance and scientific contribution to my studies.

I am deeply indebted to both Professor Akduman and Professor Yapar for their never ending enthusiasm towards scientific research and for being role models that will always guide me through my academic career.

I need to thank all members of ERG (Electromagnetic Research Group) for making the circumstances more livable and unforgettable.

I would also like to thank my mother Nilgün, my father Uğur and my sister Gizem for their invaluable moral auspices and their endless faith in me.

Finally; I would like to thank TUBITAK (the Scientific and Technological Research Council of Turkey) for supporting me financially during my master study.

June 2008 Gül Seda ÜNAL

TABLE OF CONTENTS

LIST OF FIGURES

SURFACE IMPEDANCE RECONSTRUCTION

SUMMARY

The Inverse Scattering problems related to objects having inhomogeneous impedance boundaries are addressed by considering cylindrical bodies. Two methods are presented: First, a method for the reconstruction of inhomogeneous surface impedance of a two-dimensional (2D) cylindrical object of slightly varying arbitrary shape located over a perfectly electric conducting (PEC) plane and second, a method for the impedance determination of 2D cylindrical objects located over an impedance surface. The aim of the Inverse Impedance problem is to reconstruct the inhomogeneous surface impedance of the body from the measured field data. Here, representing the scattered field as a single-layer potential leads to an ill-posed integral equation of the first kind for the density that requires stabilization for its numerical solution, for example by Truncated Singular Value Decomposition (TSVD) regularization. Then the field itself and its normal derivative on the boundary of the object, which are required for the evaluation of the surface impedance, are obtained by the use of jump relations through the Nyström method. Consequently, from the boundary condition finally the surface impedance can be reconstructed either by direct evaluation or by a minimum norm solution in the least squares sense. By considering the relation between the shape of a PEC object and its equivalent one in terms of surface impedance, it is shown that the method can also be used in the shape reconstruction. The numerical implementation shows that the method is capable of reconstructing the surface impedance as well as shape even with aspect limited data. This is due to the fact that the PEC plane has a mirror effect on the measured data which corresponds to full view configuration as in the case of objects located in an infinite medium. The reconstruction algorithm is later developed for objects located over a flat impedance surface. The numerical examples show the method is satisfactory for such kind of problems.

YÜZEY EMPEDANSI BELİRLENMESİ

ÖZET

Homojen olmayan empedans yüzeylerine sahip cisimlere ilişkin ters saçılma problemleri silindrik cisimler üzerinde incelenebilir. Bu çalışmada iki problem incelenmiştir: İlki, mükemmel iletken (PEC) yüzey üzerinde bulunan şekli hafifçe değişen iki boyutlu silindrik cisimlerin homojen olmayan yüzey empedanslarının belirlenmesi ikincisi, sabit empedans yüzeyi üzerinde bulunan şekli hafifçe değişen iki boyutlu silindrik cisimlerin homojen olmayan yüzey empedanslarının belirlenmesi. Ters empedans probleminin amacı ölçülen alan datasıyla cismin homojen olmayan yüzey empedansının belirlenmesidir. Burada, saçılan alanı tek tabakalı potansiyel ile göstererek yoğunluk için birinci çeşit kötü konumlanmış bir integral denkleme ulaşılır ki, bu denklemin sayısal çözümü için tekil nokta ayrışması (TSVD, Truncated Singular Value Decomposition) regülarizasyonu gibi bir yöntemle stabilizasyon gerekir. Daha sonra, yüzey empedansının hesabında gereken alan ve alanın cismin sınırı üzerindeki türevi sınır koşulları aracılığıyla elde edilir. Son olarak, cismin üzerindeki empedans sınır koşulundan yüzey empedansı direk çözümle ya da en küçük kareler yöntemi ile bulunur. PEC cismin şekliyle, bunun yüzey empedansı cinsinden eşdeğeri arasındaki bağlantıyı göz önüne alarak, metodun şekil bulmada da kullanılabileceği gösterilebilir. Numerik uygulamalar metodun sınırlı ölçüm datasıyla bile cismin yüzey empedansının ve şeklinin belirlenebileceğini gösterir. Bu, PEC düzlemin ölçülen data üzerinde ayna etkisi yaparak sonsuz uzayda cismin çevresinde ölçüm yapılan konfigürasyona karşı düştüğü gerçeğinden dolayıdır. Bu yöntem daha sonra empedans yüzeyi üzerinde bulunan cisimler için de genişletilmiş ve sonuçlar yöntemin bu tip problemlerin çözümünde etkili olduğunu göstermiştir.

1. INTRODUCTION

The field of inverse scattering, at least for electromagnetic waves has originated with the invention of radar and sonar during the Second World War. The ability of radar and sonar in using electromagnetic waves to determine the location of hostile objects through sea water and clouds played an important role in the outcome of the war. The success of radar and sonar inspired the possibility of not only determining the range of an object from the transmitter but also image the object and thereby identify it, e.g. to distinguish between a whale and a submarine or a goose and an airplane. The identification problem was computationally expensive and also ill-posed in the sense that the solution did not depend continuously on the measured data. The possibility of reconstruction began to appear a realistic possibility after 1970s with the development of mathematical theory of ill-posed problems by Tikhonov and others in United States together with the rise of high speed computing facilities.

Since that time the basis of electromagnetic inverse scattering problem has reached a level of maturity. The inverse scattering problem may be stated as follows: given the knowledge of the incident field and the scattered field data find the nature of the scatterer e.g. size, shape, constitutive characteristics. In recent years, the inverse scattering problems have received much attention because of their important applications in engineering areas, e.g. remote sensing, plasma diagnostics, target recognition using radar and sonar, underwater exploration, seismology, optics, etc.

An important class of problems in electromagnetic theory is the analysis of electromagnetic scattering by the buried objects [1] [2]. This is due to the fact that the results of such investigations have various applications in practice in the areas such as detection of the locations of dielectric mines, nondestructive testing, determination of underground cracks and earthquake zones, detection

of underground tunnels and pipelines, etc. Another important issue for radio frequency, microwave and remote sensing applications is the shape reconstruction of strongly scattering objects, specially metallic ones [3]. The problem consisting of finding the geometrical as well as the physical properties of inaccessible buried objects has become more attractive for researchers because of its wide range of practical applications like the observation of seismic behaviour of underground [4]. Microwave imaging methods focused on solving inverse scattering problem have proposed a complementary method of breast cancer detection, providing images of the electrical properties of tissues [5]. In many branches of applied sciences there is the need of detecting and imaging unknown objects located in inaccessible domains by solving inverse scattering problem.

One of the effective approaches used in the solution of electromagnetic scattering problems is establishment of an equivalent problem to the original one through the impedance boundary condition (IBC), which aims to reduce its mathematical and numerical complexities. IBC gives a relation between the electric and magnetic field vectors on a certain boundary in terms of a coefficient called Surface Impedance. The surface impedance is in general a tensor and may be an inhomogeneous scalar under an isotropic assumption. The Surface Impedance is commonly used to model imperfectly conducting scatterers, perfectly conducting objects coated with a penetrable or absorbing layer, and scatterers with corrugated or rough surfaces. The determination of the IBC for a given scatterer constitutes an important class of problems in the electromagnetic theory and various approximate methods have been established in the literature. In all these examples one first tries to solve the direct scattering problem for a given scattering structure and then to express the IBC in terms of electric and magnetic field on the boundary. The IBC can directly be defined either on the surface of the actual scatterer or on a fictitious boundary [6–9]. The simplest form of the IBC is the Standard Impedance Boundary Condition (SIBC) which has been used to model coatings and lossy dielectrics. Traditionally, the surface impedance appearing in SIBC is assumed to be independent of the location and associated with a constant coefficient [6] [7]. This is due to the approximations that are made in the derivation of SIBC. On the other hand, when a more accurate SIBC is

considered, the surface impedance may be a function of location, and even may be of tensor form to model anisotropic scatterers [8]. For example when the nonhomogeneous earth surface composed of different parts such as forest, rocky soil, sand, see etc. is modeled by an IBC, the surface impedance becomes a function of location. Higher order boundary conditions were also proposed for example for thick slabs where the fields vary more rapidly along the surface. The reason for going into higher order boundary conditions is to develop conditions that take into account strong variations along the surface [8–10]. On the other hand, due to the equivalence principle, the surface impedance is related to the geometrical and physical properties of the actual scatterer.

In [11] it is shown that there is an explicit relation between the geometrical variations of an arbitrary PEC object and the equivalent surface impedance placed on a circular one covering the original scatterer. Thus as long as the surface impedance is known one can extract the geometrical properties of the PEC scatterer from this information. This property can be used in the inverse scattering problems the aim of which is to determine the shape of an inaccessible PEC object from the measured scattered field. For that reason the reconstruction of the inhomogeneous surface impedance of a known boundary is of importance from both theoretical and application points of view. Recently, some effective methods have been developed in this direction [12–18].

In [12] [13] the problem of reconstruction of the surface impedance of a planar boundary with an infinite extend is analyzed by analytically continuing the measured scattered data to the boundary through Fourier transform techniques. The case of cylindrical objects of arbitrary shapes located in an infinite medium is considered in [14], and an effective method which allows one to reconstruct the surface impedance through a single illumination at a fixed frequency is developed. The method requires to collect the scattered field data all around the object. This approach is extended to the case of objects located in a half-space in [15]. Note that in this case, one achieves the reconstruction by using data which can be collected in the accessible half-space.

On the other hand, the shape reconstruction problems have been extensively investigated in the open literature and several methods based on different

approaches, such as physical optics theory, Newton-Kantorovich method, equivalent source technique and decomposition methods have been developed [18–25]. As far as we know, there is no approach which is based on the equivalent representation of the object to be reconstructed in terms of surface impedance.

In the direct scattering problem, the object and the incident wave is specified and the scattered wave is found. In contrast, in the inverse scattering problem, the scattered wave for a given incident wave is measured and the properties of the object is determined. Two considerations are important in the inverse problem. First, the measurements are normally limited and only certain quantities within some ranges are measured. Second, an effective inverse method is needed so that the object characteristics can be determined with limited measured data. Therefore, it is clear that the inverse solution may not be unique and that the existence of the solution may not be apparent. It is also common that the inverse solution is unstable, so that a slight error in the measurement may create large error in the unknown. So, if the incident and scattered waves are given, an inverse scattering problem determines the properties of the scatterer.

In this study, the 2D electromagnetic inverse scattering problem at a fixed frequency is concerned. In order to extend the method developed in [14] to the reconstruction of the surface impedance of a cylindrical object located above a perfectly conducting planar surface and use it in the shape reconstruction of PEC targets. The results of such problems may have applications in the inverse scattering problems related to objects located in the atmosphere. In such a case, the earth surface can be modeled by the perfectly conducting plane. The scattered field measurements are assumed to be established in the near field region on a circular arc. In the present study, the scattered field in the half-space above the PEC plane is represented by a single-layer potential and the density of the single-layer potential is obtained by solving the resulting Fredholm integral equation of the first kind. Since the latter one is ill-posed, a regularized solution is given via the truncated singular value decomposition scheme (TSVD). The use of the jump relations for single-layer potential leads to explicit expressions of the scattered field and its normal derivative on the impedance surface. Then the least squares reconstruction of the surface impedance is achieved by using

the SIBC itself. The surface impedance reconstruction algorithm mentioned above is also extended to the shape reconstruction of the perfectly conducting objects. To this aim the unknown object is equivalently represented in terms of a known one having a surface impedance on its boundary. Then the surface impedance is reconstructed via the method described above from the measured values of the scattered field due to the object to be reconstructed. By using the explicit expression between the surface impedance and the shape of the actual object given in [11] the determination of the shape is achieved. The method is very effective for the reconstruction of smooth and slightly varying impedances. Similar observation is valid for the application of the method to the shape reconstruction problems, e.g. it is capable of determining the shape of the PEC objects whose surfaces are relatively simple. After giving the mathematical formulation for the problem, the method is extended for the objects located over impedance surfaces which means the Green's function of the medium needs to be re-calculated.

The plan of this paper is as follows: in Section 2 the general formulation of the inverse impedance problem related to objects located over planar PEC surface is given, in addition to the numerical results, a solution is presented and the application of the method for the shape reconstruction of PEC objects is presented. While in Section 3 the inverse problem related to objects over constant impedance surface is given with the numerical results. Finally, conclusions and concluding remarks are given in Section 4.

A time factor $\exp(-i\omega t)$ is suppressed throughout this study.

2. SURFACE IMPEDANCE RECONSTRUCTION

The two-dimensional (2D) electromagnetic scattering problem illustrated in Figure 2.1 is considered. In this configuration a body D having an inhomogeneous surface impedance $Z(x)$ on its boundary ∂D is located in a homogeneous half-space bounded by perfectly conducting plane $x_2 = 0$, where $x = (x_1, x_2)$ is the position vector in R^2. It is assumed that ∂D is a smooth boundary and can also be represented in the parametric form $\partial D : \{(x_1(t), x_2(t)); t \in (0, 2\pi)\}$. The electromagnetic constitutive parameters of the background medium are ε, μ, and $\sigma = 0$. On the boundary ∂D the applicable boundary condition is the standard impedance boundary condition given by

$$-n \times (n \times E) = Z(x)\, n \times H \quad \text{on } \partial D, \tag{2.1}$$

where E and H are the total electric and magnetic field vectors and n is the outward unit normal vector of ∂D. The inverse scattering problem considered here is to reconstruct the inhomogeneous surface impedance $Z(x)$ through the measured values of the scattered field on Γ (See Figure 2.1).

To this aim the body is illuminated by a time-harmonic TM polarized plane wave whose electric field vector is

$$E^i(x) = (0, 0, u^i(x)), \quad u^i(x) = e^{-ik(x_1 \cos\phi_0 + x_2 \sin\phi_0)}, \tag{2.2}$$

where $\phi_0 \in (0, \pi)$ is the incidence angle and $k = \omega\sqrt{\varepsilon\mu}$ stands for the wave number of the background medium. Note that in such a case the total electric vector will be in the form of $E = (0, 0, u)$ and hence the problem can be formulated in terms of the scalar field function u.

2.1 The Reconstruction Algorithm

In order to formulate the problem in an appropriate way the field u^0 which is the total field in the half-space in the absence of body D is introduced. Its explicit expression can be found in any ordinary textbook,

$$u^0 = e^{-ik(x_1\cos\phi_0 + x_2\sin\phi_0)} - e^{-ik(x_1\cos\phi_0 - x_2\sin\phi_0)}. \tag{2.3}$$

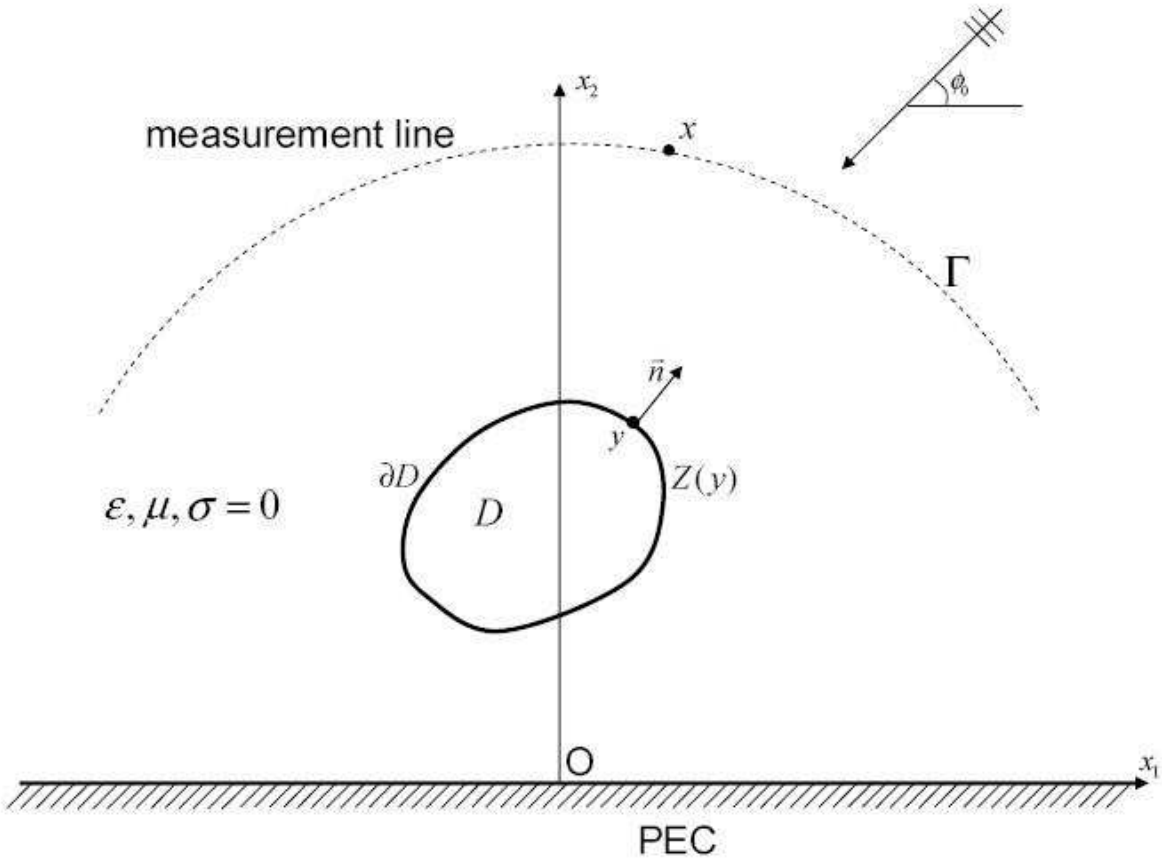

Figure 2.1: An Object with Inhomogeneous Surface Impedance over a PEC Plane

Then the difference $u^s = u - u^0$ corresponds to the scattered field due to the impedance body and satisfies the reduced wave equation

$$\Delta u^s + k^2 u^s = 0 \quad \text{in } \bar{D} \text{ and } \; x_2 > 0 \tag{2.4}$$

under the boundary conditions

$$u + \frac{\eta}{ik}\frac{\partial u}{\partial n} = 0 \quad \text{on } \partial D \tag{2.5}$$

and

$$u^s = 0 \qquad on \quad x_2 = 0 \tag{2.6}$$

with the Sommerfeld radiation condition

$$\lim_{r\to\infty} \sqrt{r}\left(\frac{\partial u^s}{\partial r}(x) - iku^s(x)\right) = 0, \quad r = |x|. \tag{2.7}$$

Here η is the normalized surface impedance defined by

$$\eta(x) := \frac{Z(x)}{Z_0}, \quad x \in \partial D$$

where $Z_0 = \sqrt{\mu/\varepsilon}$ denotes the intrinsic impedance of the background medium.

In view of 2.5 the surface impedance can be obtained from the values of the total field u and its normal derivative $\partial u/\partial n$ on ∂D via

$$\eta(x) = -ik\,\frac{u(x)}{\dfrac{\partial u}{\partial n}(x)}, \quad x \in \partial D. \tag{2.8}$$

In the sequel a method similar to one given in [14] will be described for reconstructing the required field values on the boundary ∂D from the measured scattered field data. To this aim, by the use of image theorem we first represent the scattered field as a single-layer potential of the form

$$u^s(x) = \frac{i}{4}\int_{\partial D} H_0^{(1)}(k|x-y|)\varphi(y)\,ds(y) + \frac{i}{4}\int_{\partial D'} H_0^{(1)}(k|x-y'|)\varphi(y')\,ds(y'),$$

$$x \in x_2 > 0 \tag{2.9}$$

with an unknown density function φ. Here the point $y' = (y_1, -y_2)$ is the image of the point y and $H_0^{(1)}$ is the Hankel function of the first kind with zero order. We also note that the boundary $\partial D'$ is the image of ∂D with respect to the plane $x_2 = 0$ (See Figure 2.2) and as a result of the image theorem $\varphi(y') = -\varphi(y)$.

In order to solve the surface impedance from 2.8 we need to obtain the total field u and its normal derivative $\frac{\partial u}{\partial n}$ from the given scattered field data $u^s(x),\ x \in \Gamma$. Then by substituting $u^s(x),\ x \in \Gamma$ into 2.9 the problem can be reduced to the solution of the following Fredholm integral equation of the first kind

$$A\varphi = u^s(x), \quad x \in \Gamma \tag{2.10}$$

for the density φ, where the integral operator A is given by

$$(A\varphi)(x) := \frac{i}{4}\int_{\partial D} H_0^{(1)}(k|x-y|)\varphi(y)\,ds(y) + \frac{i}{4}\int_{\partial D'} H_0^{(1)}(k|x-y'|)\varphi(y')\,ds(y'). \tag{2.11}$$

The operator A has an analytic kernel and therefore the equation 2.10 is severely ill-posed. For that reason some kind of stabilization has to be applied. Here we obtain a regularized solution by using Singular Value Decomposition (SVD). For a linear compact operator A, the SVD is defined as triple $\{\Psi_n, \sigma_n, \upsilon_n\}$ such that

$$A\varphi = \sum_{n=-\infty}^{\infty} \sigma_n\,(\varphi, \psi_n)\,\nu_n \tag{2.12}$$

which leads to the explicit inversion formula

$$\varphi = \sum_{n=-\infty}^{\infty} \frac{1}{\sigma_n}\,(u^s, \nu_n)\,\psi_n. \tag{2.13}$$

Due to the properties of the kernel of the operator A, the singular values σ_n accumulate to zero exponentially fast for $n \to \infty$. A possible way to tackle this instability is given by the regularized solution provided by TSVD inversion formula

$$\varphi = \sum_{n=-N}^{N} \frac{1}{\sigma_n}\,(u^s, \nu_n)\,\psi_n \tag{2.14}$$

in which the truncation index N is usually determined on the basis of the expected measurement noise.

Once the single-layer density φ is known, the values u and $\partial u/\partial n$ of the total field on the boundary ∂D can be recovered through the jump relations for the single-layer potential [18], that is, by

$$u(x) = u^0(x) + \frac{i}{4}\int_{\partial D} H_0^1(k|x-y|)\,\varphi(y)\,ds(y) + \frac{i}{4}\int_{\partial D'} H_0^1\left(k|x-y'|\right)\varphi\left(y'\right)ds\left(y'\right)$$

$$x \in \partial D \tag{2.15}$$

and

$$\frac{\partial u}{\partial n}(x) = \frac{\partial u^0}{\partial n}(x) + \frac{i}{4}\int_{\partial D} \frac{\partial H_0^{(1)}(k|x-y|)}{\partial n(x)}\,\varphi(y)\,ds(y) + \frac{i}{4}\int_{\partial D'} \frac{\partial H_0^{(1)}(k|x-y'|)}{\partial n(x)}\,\varphi(y')\,ds(y')$$

$$-\frac{1}{2}\,\varphi(x), \quad x \in \partial D \tag{2.16}$$

For the numerical evaluation of these singular integrals over ∂D we make use of the same quadrature formulas in connection with the Nyström method [26].

The surface impedance can now be reconstructed from 2.8 in terms of the values of u and its normal derivative for each point $x \in \partial D$. It is obvious that this solution will be sensitive to errors in the normal derivative of u in the vicinity of zeros. To obtain a more stable solution, we express the unknown impedance function in terms of some basis functions ϕ_n, $n = 1,\ldots,M$, as a linear combination

$$\eta = \sum_{n=1}^{M} a_n \phi_n \quad \text{on } \partial D. \tag{2.17}$$

A possible choice of basis functions consists of splines or trigonometric polynomials. Then we satisfy 2.8 in the least squares sense, that is, we determine the coefficients $a_1,\ldots,a_M$ in 2.17 such that for a set of grid points $x_1,\ldots,x_M$ on ∂D the least squares sum

$$\sum_{m=1}^{M} \left| u(x_m) + \sum_{n=1}^{M} a_n \phi_n(x_m) \frac{\partial u}{\partial n}(x_m) \right|^2 \tag{2.18}$$

is minimized. The number of basis functions M in (2.17) can be considered as some kind of regularization parameter.

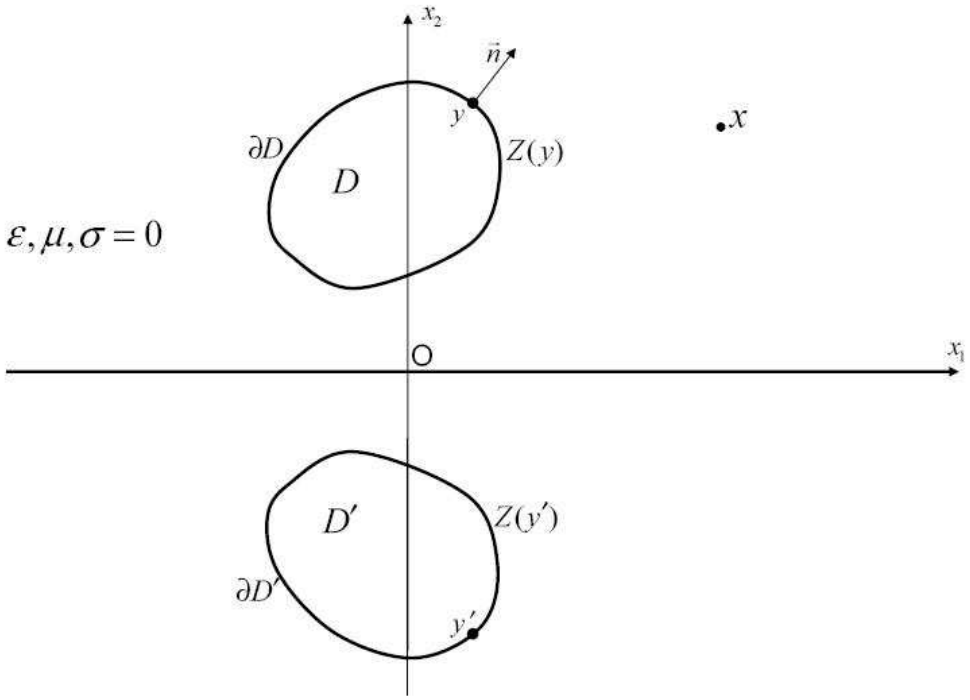

Figure 2.2: Image of the Object D

2.2 Application to Shape Reconstruction of Conducting Objects

In [11] it is shown that there is an explicit relation between the shape of a PEC object and its equivalent surface impedance defined on a fictitious boundary which is assumed to cover the actual one. By considering this property the reconstructed surface impedance can be used for the shape determination of the PEC objects. To this aim, we consider a circular domain which covers the perfectly conducting object to be reconstructed and set an equivalent problem by imposing an inhomogeneous surface impedance $Z(\phi)$ on the new circular boundary (See Figure 2.3). If the object has a slightly varying and smooth boundary, it can be represented in terms of a Standard Impedance Boundary Condition [11] and the following relation is valid between surface function $f(t) = \sqrt{x_1(t)^2 + x_2(t)^2}$ of the PEC object and parametric form of equivalent surface impedance $Z(t)$ on the circular boundary $\rho = a$, namely,

$$Z(t) = i\omega\mu_0(f(t) - a), \qquad t \in (0, 2\pi). \tag{2.19}$$

Then, for the given measured scattered data related to the actual object, we first reconstruct the surface impedance $Z(t)$ via the method given in previous section then obtain the surface function $f(t)$ simply from 2.19.

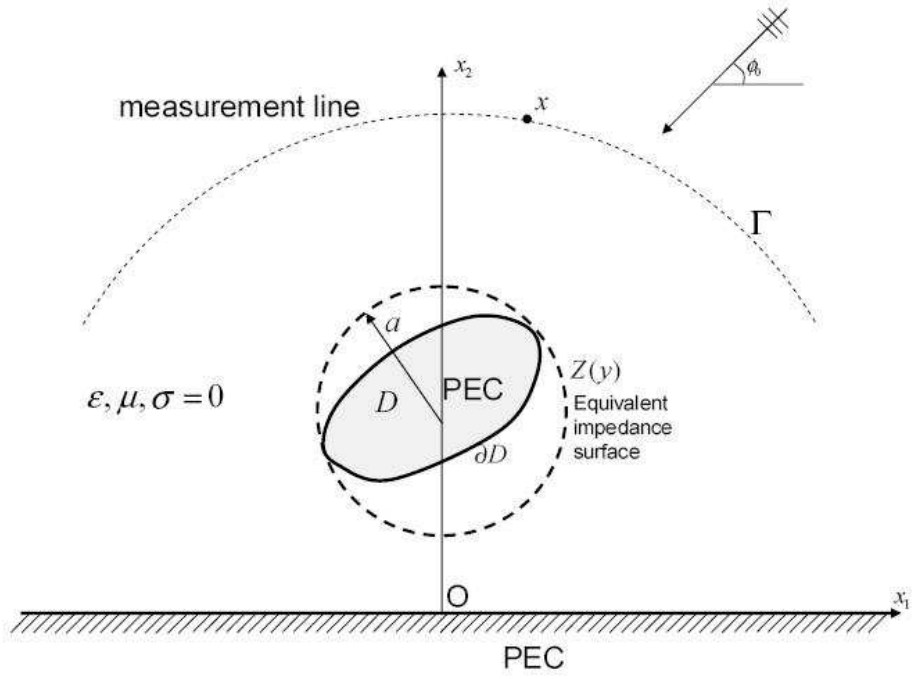

Figure 2.3: PEC Object with Arbitrary Geometry and its Equivalent one in terms of Surface Impedance

2.3 Numerical Results

In this section some illustrative examples both for surface impedance determination and its use in the shape reconstruction are presented. The data which should be collected by real measurements are created synthetically by solving the associated scattering problem through the mixed layer potential approach [26]. In all numerical examples the frequency of the incident wave is chosen as $f = 300MHz$ and the background as free space corresponding to a wavelength $\lambda = 1m$. A random noise of level 1% is added to the simulated data for each example. In particular, a random term $n_l|u^s|e^{2ir_d\pi}$ is added to each scattered field value u^s, n_l being the noise level and r_d a random number between 0 and 1. In the application of the least squares solution the basis functions are chosen as combinations of $\cos(2\pi p\phi)$ and $\sin(2\pi p\phi)$, $p = 0, 1, \ldots, P$, and the number P is determined by trial and error.

As a first example a drop-shaped object given by the parametric equation

$$\partial D = \{(0.4\cos t, 0.5 + 0.2\sin(t/2)) : t \in [0, 2\pi]\} \tag{2.20}$$

and having a surface impedance with real and imaginary parts as shown in Figure 2.4a and Figure 2.4b, respectively (solid line). Their reconstructed values are also illustrated in the same figures (dashed lines). In particular the body is illuminated by a plane wave with an illumination angle of $\phi_0 = \pi/2$. The reconstruction is obtained for the scattered data observed on the semi circle $R = 5m$ at 100 points. The number of singular values used in the TSVD inversion is $N = 15$ and the number of basis functions used in Least Squares Optimization is $P = 9$. The exact and reconstructed surface impedance variations are in a very good agreement for this example. This is because, although the data is observed in a limited domain $\phi \in (0, \pi)$ on a semi-circle $R = 5, \quad x_2 > 0$, due to the *mirror effect* of the $x_2 = 0$ plane, the measured data contains information also from the shadow part of the object, which allows us to have a full view configuration.

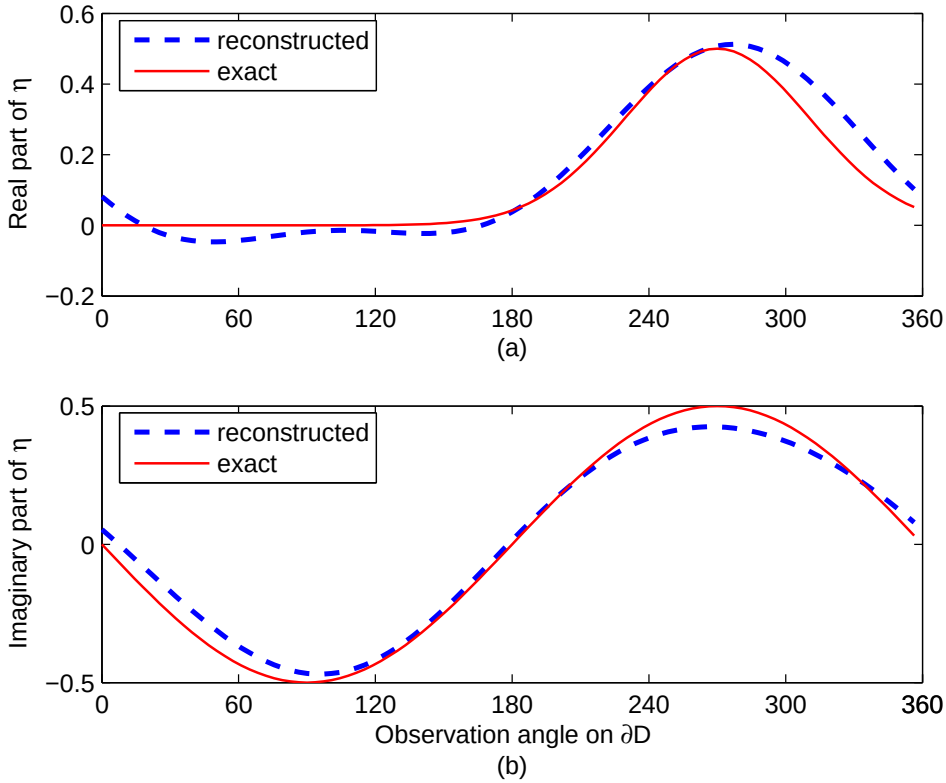

Figure 2.4: Normalized Exact and Reconstructed Values of the Real and Imaginary Parts of a Surface Impedance on a Drop Shaped Object

In order to give an idea about the effect of the extend of the measurement domain, a kite-shaped object with parametric equation

$$\partial D = \{(0.2\cos t + 0.1\cos 2t - 0.032, 0.5 + 0.2\sin t) : t \in [0, 2\pi]\} \tag{2.21}$$

is taken into account and the reconstructions are obtained for three different measurement domains $\phi \in (\pi/4, 3\pi/4)$, $\phi \in (\pi/6, 5\pi/6)$ and $\phi \in (0, \pi)$ on the semi-circle $R = 5, \quad x_2 > 0$. The real and imaginary parts of the exact and reconstructed surface impedances are demonstrated in Figure 2.5a and Figure 2.5b, respectively. In all cases, the parameters are chosen as $\phi_0 = \pi/2$, $N = 11$ and $P = 5$. As expected the aspect limited measurement configuration yields poor reconstructions when the measurement domain getting smaller. Nevertheless, the method is capable of determining surface impedance of a given scatterer through the measurement of the scattered field for single illumination at a fixed frequency when the impedance function has a smooth variation.

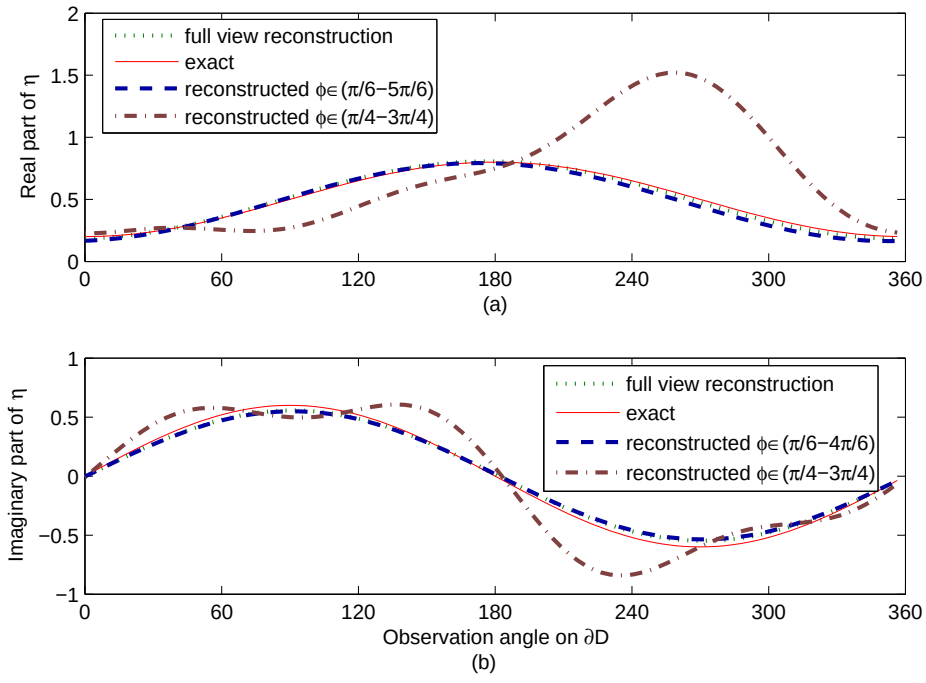

Figure 2.5: Normalized Exact and Reconstructed Values of the Real and Imaginary Parts of a Surface Impedance on a Kite Shaped Object

The use of reconstructed surface impedance in the shape reconstruction applications is tested by first considering a perfectly conducting object with parametric equation,

$$\partial D = \{(0.4+0.02\cos(8t))\cos(t), 2+(0.4+0.02\sin(8t))\sin(t) : t \in [0,2\pi]\}. \quad (2.22)$$

The scattered field measurements due to this object is assumed to be performed on the semi circle $R = 5$, $\phi \in (0,\pi)$. The equivalent impedance boundary is chosen as the circle with radius $a = 0.42$ and center $(0,2)$ and the surface impedance is reconstructed on this circle from above given data. By using the relation (2.19) the shape of the object is reconstructed. In Figure 2.6 the variation of the exact and reconstructed values of the surface impedance on the circle $R = 5m$ are given. The exact and reconstructed shapes of the object are illustrated in Figure 2.7. As can easily be observed the reconstructed shape is very close to the actual one. Note that in this example the variation of the surface is very small compared to wavelength.

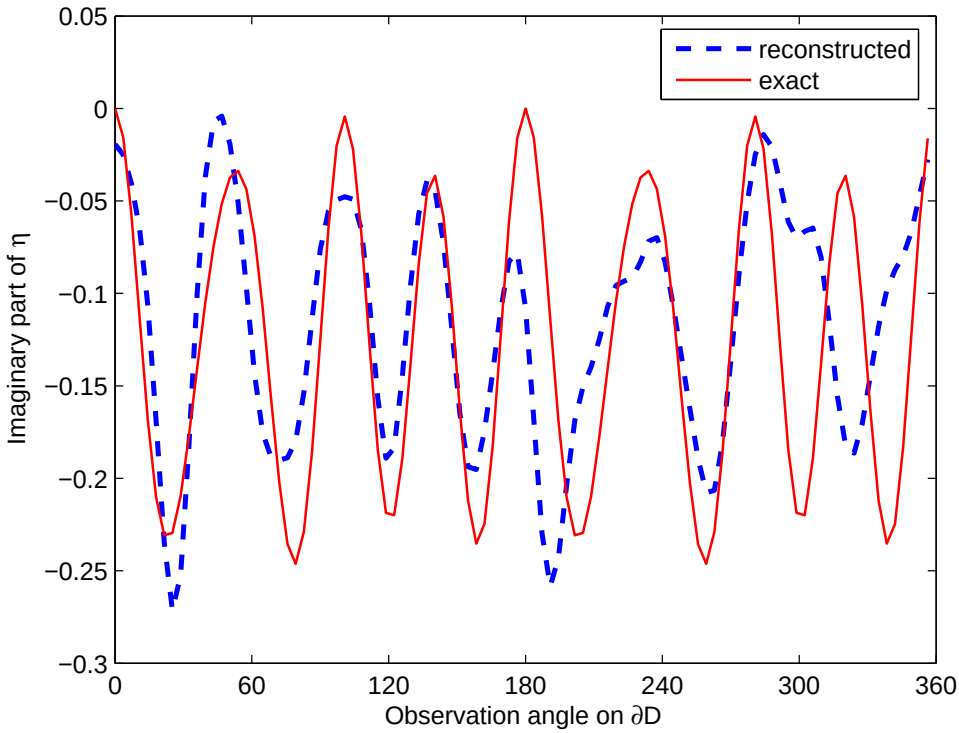

Figure 2.6: Exact and Reconstructed Normalized Equivalent Surface Impedance on the circle $a = 0.42m$ for the Perfectly Conducting Object given in Equation 2.22.

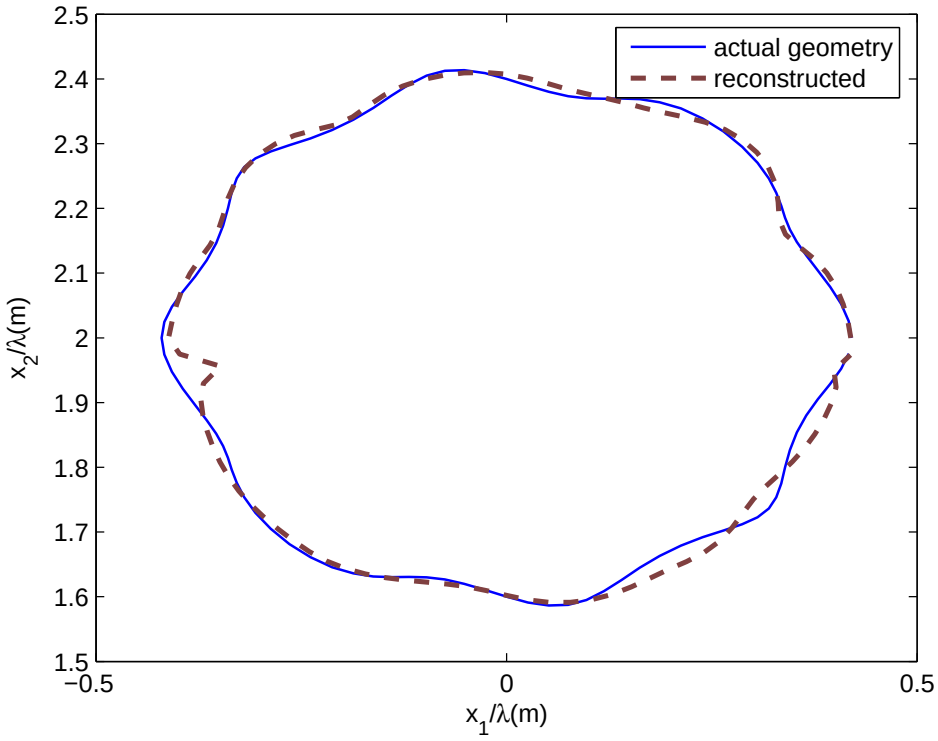

Figure 2.7: Exact and Reconstructed Shapes of the Object given in Equation 2.22.

For a different object of parametric equation

$$\partial D = \{(0.3+0.05\cos(3t))\cos(t), 2+(0.3+0.05\sin(3t))\sin(t) : t \in [0,2\pi]\} \quad (2.23)$$

exact and reconstructed surface impedances are given in Figure 2.8 while the exact and reconstructed shapes are demonstrated in Figure 2.9. Obviously, very accurate reconstructions are obtained.

The last two examples show that the surface impedance concept can be used for the shape reconstruction of the perfectly conducting objects. The quality of the reconstructions is related to the oscillations on the surface variation of the object to be reconstructed and the method is not capable of reconstructing objects of complex shapes having large number of concave and convex parts. This is due to the fact that the method for surface impedance reconstruction is valid for those impedances having smooth variation and Standard IBC modeling is used.

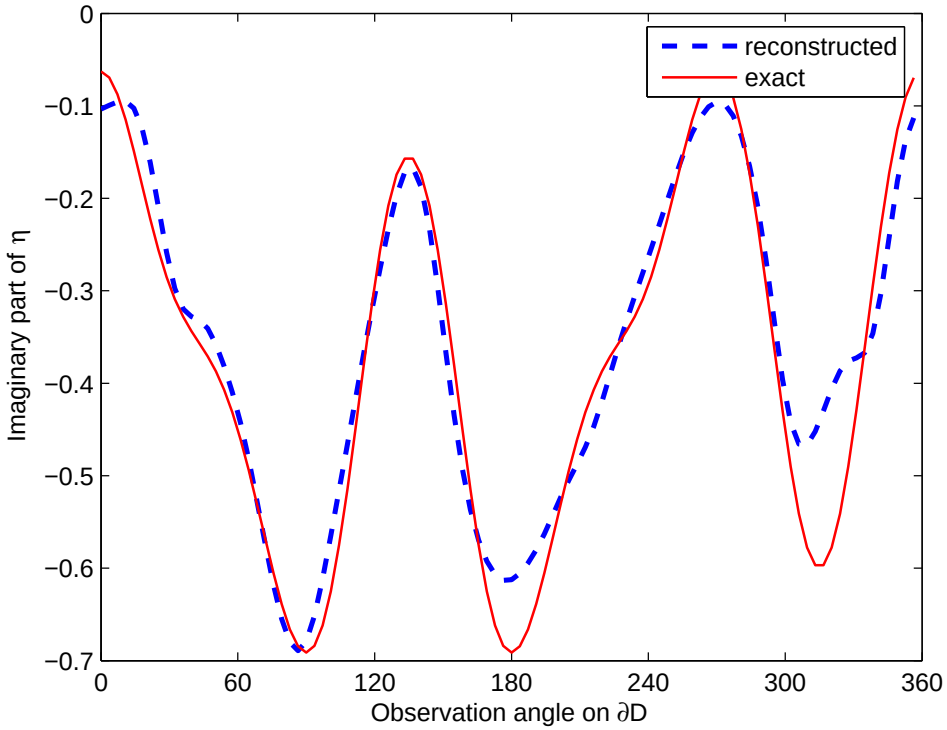

Figure 2.8: Exact and Reconstructed Equivalent Surface Impedance on the circle $a = 0.32m$ for the Perfectly Conducting Object given in Equation 2.23.

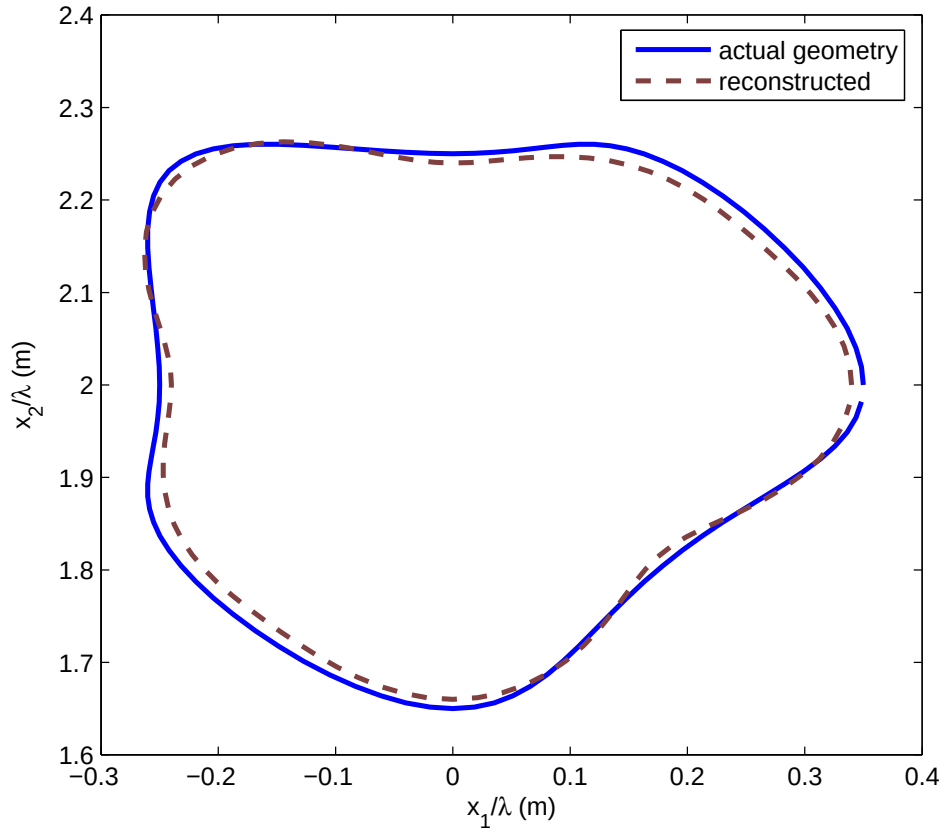

Figure 2.9: Exact and Reconstructed Shapes of the Object given in Equation 2.23.

3. CONSTANT IMPEDANCE SURFACE

A method is presented for the reconstruction of inhomogeneous surface impedance of a two dimensional (2D) cylindrical object of arbitrary shape located over a constant impedance plane. The method is an extension of the one given above. The impedance surface is illuminated with a time harmonic plane wave and the measurements are performed on a circular arc in the half space above the surface. The scattered field in the whole half-space is then represented by a single-layer potential where the unknown single-layer potential density is obtained by solving the resulting Fredholm integral equation of the first kind. A regularized solution can be obtained using Singular Value Decomposition (SVD). Once the single layer density is known the total field and the normal derivative of the total field on the boundary of the cylindrical object through jump relations for single layer potential. For the numerical evaluation of the singular integral, Nyström Method is used. The surface impedance later can be reconstructed using Standard Impedance Boundary Condition (SIBC).

3.1 Green's Function of the Medium

The Green's function, also known as the source function or influence function, is the kernel function obtained from a linear boundary value problem and forms the essential link between the differential and integral formulations. To obtain the field caused by a distributed source by the Green's function technique, the effects of each elementary portion of source have to be found and summed up. If $G(x;y)$ is the field at the observation point (or field point) x caused by a unit point source at the source point y, then the field at x by a source distribution $g(y)$ is the integral of $g(y)G(x;y)$ over the range of y occupied by the source. The function G is the Green's function. Thus, physically, the Green's function $G(x;y)$ represents the potential at x due to a unit point charge at y.

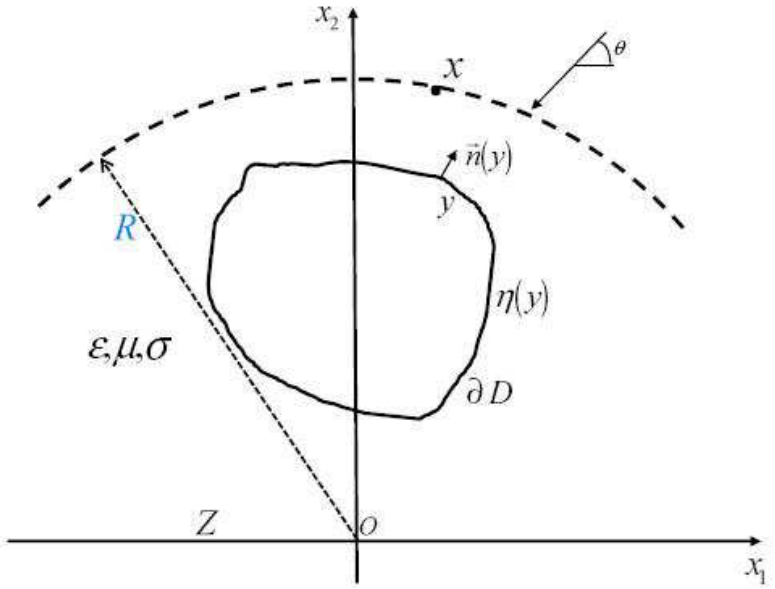

Figure 3.1: An object with Inhomogeneous Surface Impedance over a Constant Impedance Plane

Consider a linear operator L that operates on a function of x and y. If we wish to solve the equation

$$L(x,y) = S(x,y) \tag{3.1}$$

we first solve

$$LG(x_1,y_1|x_2,y_2) = \delta(x_1-x_2)\delta(y_1-y_2) \tag{3.2}$$

and determine the Green's function G for the operator L. For this problem, 3.1 is

$$\Delta u + k^2 u = 0 \quad \text{in } \bar{D} \text{ and } \; x_2 > 0 \tag{3.3}$$

which means the equation needs to be solved in order to obtain Green's function is

$$\Delta G + k^2 G = -\delta(x_1-y_1)\,\delta(x_2-y_2)\,. \tag{3.4}$$

An efficient way of obtaining the Green's function is by means of Fourier series expansion;

$$\hat{G}(\upsilon, x_2; y) = \int_{-\infty}^{\infty} G(x_1, x_2; y)\, e^{-i\upsilon x_1} dx_1 \tag{3.5}$$

which leads us to

$$\frac{\partial^2 \hat{G}}{\partial x_2^2} - \left(\upsilon^2 - k^2\right) \hat{G} = -e^{-i\upsilon y_1}\, \delta\left(x_2 - y_2\right) \tag{3.6}$$

by taking Fourier transform of 3.4.

Here, representing the $\hat{G}$ as

$$\hat{G}(\upsilon, x_2; y) = \left\{ \begin{array}{ll} Ae^{-\gamma x_2}, & x_2 > y_2 \\ Be^{-\gamma x_2} + Ce^{\gamma x_2}, & 0 < x_2 < y_2 \end{array} \right\} \tag{3.7}$$

and solving under conditions

$$\hat{G}\Big|_{x_2 \to y_2^+} - \hat{G}\Big|_{x_2 \to y_2^-} = 0 \tag{3.8}$$

and

$$\frac{\partial \hat{G}}{\partial x_2}\Big|_{x_2 \to y_2^+} - \frac{\partial \hat{G}}{\partial x_2}\Big|_{x_2 \to y_2^-} = -e^{-i\upsilon y_1} \tag{3.9}$$

and impedance boundary condition

$$\hat{G} + \frac{\eta}{ik} \frac{\partial \hat{G}}{\partial x_2}|_{x_2=0} = 0 \tag{3.10}$$

gives the Fourier transform of the Green's function as

$$\hat{G}(\upsilon, x_2; y) = \frac{1}{2\gamma} e^{-\gamma(x_2 - y_2)} e^{-i\upsilon y_1} - \frac{1}{2\gamma} e^{-\gamma(x_2 + y_2)} e^{-i\upsilon y_1} - \frac{Z}{1 - \gamma Z} e^{-\gamma(x_2 + y_2)} e^{-i\upsilon y_1},$$

$$x_2 > 0 \tag{3.11}$$

After obtaining the Green's function by taking the inverse Fourier transform of the 3.11 the reconstruction algorithm given in 2.1 is used to determine the surface impedance related to objects above impedance surfaces.

3.2 The Total Field

The field u_0 which is the total field in the half space above the constant impedance surface in the absence of the body D needs to be solved. It can be represented as

$$u^0(x) = e^{-ik(x_1\cos\theta + x_2\sin\theta)} + Re^{-ik(x_1\cos\theta - x_2\sin\theta)} \tag{3.12}$$

where R, the reflection coefficient is

$$R = \frac{ik\sin\theta\cdot Z - 1}{ik\sin\theta\cdot Z + 1} \tag{3.13}$$

which is determined using the SIBC

$$u^0(x) + \frac{\eta}{ik}\frac{\partial u^0(x)}{\partial x_2}|_{x_2=0} = 0 \tag{3.14}$$

Here $Z = \eta/ik$.

3.3 Numerical Results

The inverse scattering problem whose aim is to reconstruct the surface impedance of a cylindrical object located over a constant impedance plane is solved. The method yields satisfactory surface impedance reconstructions for a single wave illumination. The frequency of the incident wave is chosen as $f = 300MHz$ and the background as free space corresponding to a wavelength $\lambda = 1m$. In the application of the least squares solution the basis functions are chosen as combinations of $\cos(2\pi p\phi)$ and $\sin(2\pi p\phi)$, $p = 0,1,\ldots,P$, and the number P is determined by trial and error.

As an example an ellipse-shaped object given by the parametric equation

$$\partial D = \{(0.3\cos t, 0.5 + 0.1\sin(t)) : t \in [0, 2\pi]\} \tag{3.15}$$

and having a surface impedance with real and imaginary parts as shown in Figure 3.2a and Figure 3.2b, respectively. Their reconstructed values are also illustrated in the same figures (dashed lines). In particular the body is illuminated by a plane wave with an illumination angle of $\phi_0 = \pi/2$. The body is located over an impedance surface where $Z = 5$. The reconstruction is obtained for the scattered

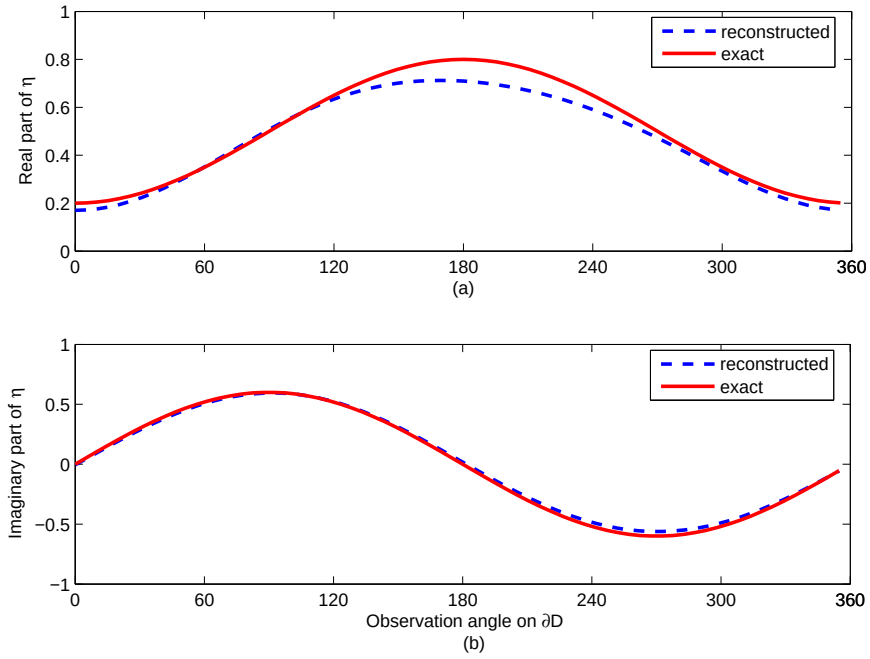

Figure 3.2: Exact and Reconstructed Shapes of the Object given in Equation 3.15.

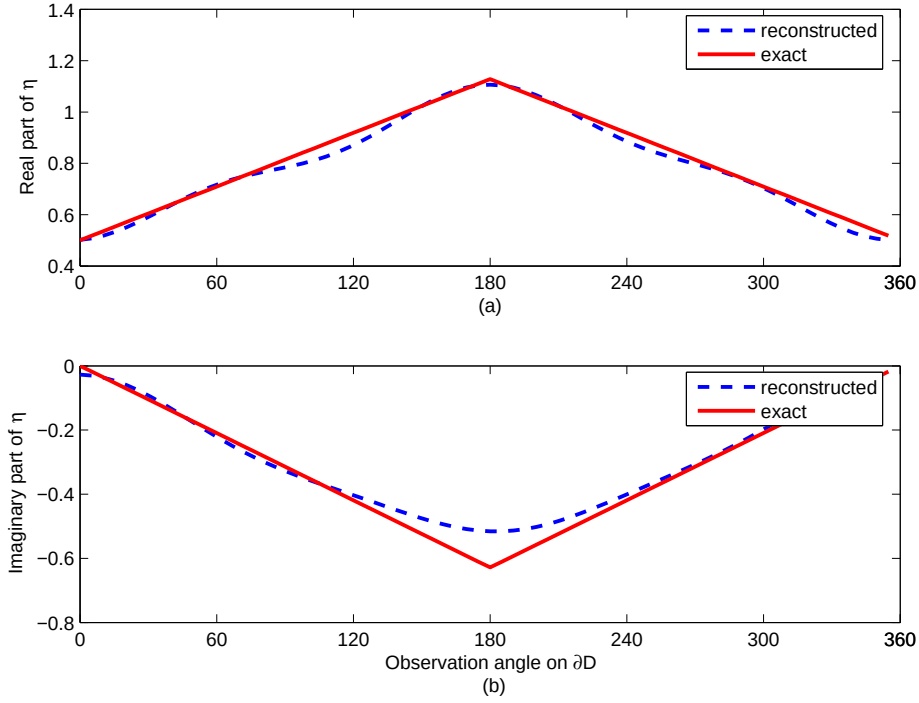

Figure 3.3: Exact and Reconstructed Shapes of the Object given in Equation 3.16.

data observed on the semi circle $R = 5m$ at 120 points. The number of singular values used in the TSVD inversion is $N = 20$ and the number of basis functions used in Least Squares Optimization is $P = 5$. The exact and reconstructed surface impedance variations are in a very good agreement for this example.

Another example for a box-shaped object given by the parametric equation

$$\partial D = \left\{ (0.2(\cos t)^3 + \sin(t), 2 + 0.2(\sin(t))^3 + \sin(t)) : t \in [0, 2\pi] \right\} \tag{3.16}$$

which is located over an impedance surface $Z = 10$ and illuminated by a plane wave $\phi_0 = \pi/4$ where the reconstruction is obtained on a semi-circle $R = 5m$ at 140 points and the number of singular values used in the TSVD inversion is $N = 30$ and the number of basis functions used in Least Squares Optimization is $P = 4$ shows the method has quite satisfactory results as shown in Figure 3.3a and 3.3b.

4. CONCLUSION

The inverse scattering problem whose aim is to reconstruct the surface impedance of a cylindrical object of arbitrary shape over a PEC plane is solved through the extension of the method in [8]. On the other hand, by means of the equivalency theorem, it is possible to show that a PEC object can be represented in terms of a surface impedance defined on a known surface and the surface impedance is explicitly related to the shape of the actual object. By the use of this result the method can also be used in the shape reconstruction problems related to PEC bodies. The method later extended to objects located over impedance surfaces.

The method yields quite satisfactory surface impedance reconstructions for a single illumination even in the case of aspect limited data. This is due to the fact that the planar PEC boundary reflects all the field which carries the information about the non-illuminated part of the object. In other words, the reflection of the incident field from the PEC plane behaves like a second excitation and interacts with the shadow part of the object. When the surface impedance equivalently represents a PEC object, it yields quite accurate shape reconstructions for slightly varying object boundaries. This is the result of using only standard impedance boundary condition for the equivalent problem. By using higher order IBC, it may be possible to reconstruct more complex shapes. Future studies are devoted in this direction.

The satisfactory results for the object located over impedance surface shows that the method is useful in the reconstruction even for the constant impedance case. For this configuration, the added term in the Green's function is because of the losses caused by the impedance surface.

REFERENCES

[1] **Altuncu, Y.**, **Yapar, A. and Akduman, I.**, 2006. On the Scattering of Electromagnetic Waves by Bodies Buried in a Half-Space with Locally Rough Interface, *IEEE Trans. Geoscience and Remote Sensing*, **44**, 1435–1443.

[2] **Altuncu, Y.**, **Akduman, I. and Yapar, A.**, 2007. Detecting and Locating Dielectric Objects Buried Under a Rough Interface, *IEEE Geoscience and Remote Sensing Letters*, **4**, 251–255.

[3] **Pieri, R.**, **Liseno, A.**, **Solimene, R. and Soldovieri, F.**, 2006. Beyond Physical Optics SVD Shape Reconstruction of Metallic Cylinders, *IEEE Trans. Antennas and Propagation*, **54**, 655–665.

[4] **Akduman, I. and Pothast, R.**, 2002. Finding the location and shape pf buried obstacles using acoustic or electromagnetic waves, *Journal of Comp. and Appl. Math.*

[5] **Fear, E. and Stuchly, M.**, 2000. Microwave detection of breats cancer: a study of tumor response variations, *Proceedings of 22th Annual EMBS International Conference*, 74–77.

[6] **D.J.Hoppe and Rahmat-Samii, Y.**, 1995. Impedance Boundary Conditions in Electromagnetics, Taylor and Francis, London.

[7] **Senior, T. and Volakis, J.**, 1995. Approximate Boundary Conditions in Electromagnetics, Institutions of Electrical Engineers, London.

[8] **Senior, T.**, **Volakis, J. and Legualt, S.**, 1997. Higher Order Impedance and Absorbing Boundary Conditions, *IEEE Trans. Antennas and Propagation*, **45**, 107–14.

[9] **Marceaux, O. and Stupfel, B.**, 2000. Higher order impedance boundary conditions for multilayer coated 3D objects, *IEEE Trans. Antennas and Propagations*, **46**, 429–36.

[10] **Wang, H.**, 1987. A simple conservative difference scheme for solving full Euler equations, *Chinese Journal Computational Physics*, **4**, 79–84.

[11] **Ozdemir, O.**, **Akduman, I.**, **Yapar, A. and Crocco, L.**, 2007. Higher Order inhomogeneous impedance boundary conditions for perfectly conducting object, *IEEE Trans. Geosciences and Remote Sensing*, **45**, 1291–7.

[12] **Yapar, A. and Akduman, I.**, 2001. Reconstruction of the surface impedance of an inhomogenous impedance boundary beyond layered media, *Radio Science*, **36**, 539–51.

[13] **Akduman, I. and Yapar, A.**, 2001. Surface impedance determination of a planar boundary by the use of scattering data, *IEEE Trans. Antennas and Propagation*, **49**, 304–1.

[14] **Akduman, I. and Kress, R.**, 2003. Direct and Inverse Scattering problems for inhomogenous impedance cylinders of arbitrary shape, *Radio Science*, **38**, 1055.

[15] **Sahinturk, H.**, 2004. On the reconstruction of inhomogenous surface impedance of cylindrical bodies, *IEEE Trans. Magnetics*, **40**, 1152–5.

[16] **Kress, R. and Rundell, W.**, 2001. Inverse scattering for shape and impedance, *Inverse Problems*, **17**, 1075–85.

[17] **Cakoni, F. and Colton, D.**, 2004. The determination of the surface impedance of a partially coated obstacle from far field data, *SIAM J. Appl. Math.*, **64**, 709–23.

[18] **Colton, D.**, **Haddar, H. and Piana, M.**, 2003. The linear sampling method in inverse scattering theory, *Inverse Problems*, **19**, 105–38.

[19] **Qing, A.**, **Lee, C.K. and Jen, L.**, 2001. Elecromagnetic inverse scattering of two-dimensional perfectly conducting objects by real-coded genetic algorithm, *IEEE Trans. Geoscience and Remote Sensing*, **39**, 665–76.

[20] **Bojarski, N.**, 1982. A survey of the physical optics inverse scattering identity, *IEEE Trans. Antennas and Propagation*, **30**, 980–9.

[21] **Liu, C. and Kiang, Y.**, 1996. Inverse scattering for conductors by the equivalent source method, *IEEE Trans. Antennas and Prop*, **44**, 310–6.

[22] **Belkebir, K.**, **Kleinmann, R. and Pichot, C.**, 1997. Microwave imaging-location and shape reconstruction from multifrequency scattering data, *IEEE Trans. Microwave Theory Tech.*, **45**, 469–76.

[23] **Colton, D. and Kress, R.**, 2006. Using fundamental solutions in inverse scattering, *Inverse Problems*, **22**, 49–66.

[24] **Kress, R.**, 2003. Newton's method for inverse obstacle scattering meets the method of least squares, *Inverse Problems*, **19**, 91–104.

[25] **Pieri, R.**, **Liseno, A. and Soldovieri, F.**, 2001. Shape reconstruction from PO multifrequency scattered fields via the singular value decomposition approach, *IEEE Trans. Antennas and Propagation*, **49**, 1333–43.

[26] **Colton, D. and Kress, R.**, 1999. Inverse Acoustic and Electromagnetic Scattering Theory, Springer-Verlag, Berlin Heidelberg New York.

CIRCULUM VITAE

Gül Seda Ünal was born in Ankara, Turkey in 1983. She received her B.Sc. degree in Telecommunications Engineering from Istanbul Technical University in 2006. She started working towards M.Sc. degree in Telecommunications Engineering Program of Institute of Science and Technology at Istanbul Technical University.